In memory of T. A. Stephenson

A Two-dimensional Nuclear Magnetic Resonance Exchange Study of the Fluxionality of [$PtIMe_3(MeSCH_2CH_2SEt)$]†

Edward W. Abel, Ian Moss, Keith G. Orrell,* Vladimir Šik, and David Stephenson
Department of Chemistry, The University, Exeter, Devon EX4 4QD

Two-dimensional n.m.r. exchange spectroscopy has been used to measure the kinetics of four-site exchange associated with pyramidal sulphur inversion in the complex [$PtIMe_3(MeSCH_2CH_2SEt)$]. Ethyl sulphur inversion occurs more readily than methyl sulphur inversion with $\Delta G^{\ddagger}$ values for the processes differing by 3.3—7.2 kJ mol^{-1} depending on which pathways are considered. Application of the same n.m.r. method to the three-site exchange of the Pt-methyl groups has led to $\Delta G^{\ddagger}$ values of 90.9 ± 0.5, 92.6 ± 0.4, and 97.7 ± 1.9 kJ mol^{-1}. The first two values are attributed to ligand (180°)/$PtMe_3$ (120°) correlated rotations, the different values depending on which equatorial Pt-methyl group is interchanged. The third $\Delta G^{\ddagger}$ value, arising from direct exchange of the two equatorial Pt-methyl environments, refers to independent ligand rotation and/or Pt-methyl scrambling.

The stereodynamics of transition metal complexes of co-ordinated sulphur ligands have been extensively investigated by total bandshape analysis of variable-temperature n.m.r. spectra.[1] This so-called dynamic n.m.r. (d.n.m.r.) technique,[2] although very powerful, suffers from certain limitations. For instance, it cannot measure exchange rates which are too slow substantially to affect n.m.r. bandshapes, and furthermore, it is not easily applied to n-site exchange problems, where $n > 3$, because of the difficulty of fitting exchange-broadened spectra to unique sets of n exchange rate constants. Both these restrictions can be alleviated by using either the Forsén–Hoffman spin saturation transfer method[3,4] or the technique of two-dimensional exchange spectroscopy (2D-EXSY) based on the Jeener 2D-NOESY pulse sequence.[5,6] The magnetisation transfer technique, the theory of which has recently been generalised for n-site exchanges,[7,8] involves a series of double-irradiation experiments and, in practice, requires that the spin-lattice relaxation times of the nuclei at each site be assumed equal. The 2D-EXSY method[9–11] requires no such assumption regarding T_1 values, magnitudes of which need be only approximately known. Furthermore, under favourable circumstances *all* rate constants can be uniquely determined by a *single* two-dimensional experiment, and additionally the experiment can be performed even in cases of small chemical shift dispersion of individual resonances. We have recently shown that this method is quantitatively reliable for three-site exchange systems, as exemplified by the slow-exchange ^{195}Pt spectra of the invertomers of the complexes [$PtXMe_3(MeSCH_2CH_2SMe)$] (X = Cl or I).[11]

We now wish to demonstrate further the power of the 2D-EXSY method for quantitative kinetic studies by describing the dynamic spectral analysis of the complex [$PtIMe_3(MeSCH_2CH_2SEt)$]. The stereodynamics of this complex are intractable by conventional one-dimensional n.m.r. bandshape methods, since at low temperatures, where sulphur inversion is occurring at moderate rates, the exchange-broadened spectra are sensitive to at least four independent exchange rate constants, and at high temperatures, the ligand and trimethylplatinum fluxions are described by a further three rate constants.

† *Non-S.I. unit employed:* mmHg ≈ 133 Pa.

In this paper we will demonstrate how all these rates and associated activation energies can be reliably measured by 2D-EXSY experiments. The chemical importance of the study lies in the precise measurement of the alkyl dependence of S-alkyl pyramidal inversion, and the greater insight provided by the two-dimensional, compared to the one-dimensional, n.m.r. approach into the mechanisms of the various fluxional processes.

Experimental

Materials.—Preparation of 2,5-Dithiaheptane. Sodium metal (3.5 g, 0.15 mol) was dissolved in methanol (250 cm^3) under nitrogen, and ethanethiol (9.3 g, 0.15 mol) was then added quickly to the solution *via* a pressure-equalising dropping funnel. The mixture was stirred at room temperature for 1 h, and 2-chloroethyl methyl sulphide (16.8 g, 0.15 mol) added dropwise over a period of 30 min. The mixture was stirred for 16 h, after which time the volume of the solution was reduced to *ca.* 50 cm^3 by rotary evaporation. After filtration, the product was isolated by distillation at reduced pressure, the fraction boiling at 75—76 °C (0.1 mmHg pressure) being collected. The yield of 2,5-dithiaheptane was 7.8 g (38.0%). ^1H N.m.r. ($CDCl_3$ solution): δ 1.25 (t, CH_3CH_2S, $^3J_{HH}$ = 7.46), 2.13 (s, CH_3S–), 2.55 (q, CH_3CH_2S–, $^3J_{HH}$ = 7.46 Hz), 2.72 (s, –SCH_2CH_2S–).

Preparation of (2,5-Dithiaheptane)iodotrimethylplatinum(IV). —[$(PtIMe_3)_4$] (0.401 g, 0.28 mmol) and 2,5-dithiaheptane (0.2 cm^3) were heated under reflux for 3 h in $CHCl_3$ (*ca.* 50 cm^3). After cooling and removal of solvent at reduced pressure, the colourless oil obtained was extracted with hexane (10 cm^3) to remove excess ligand. Recrystallisation of the residue from chloroform–hexane afforded colourless crystals of [$PtIMe_3(MeSCH_2CH_2SEt)$] {0.302 g, 53.7% yield, relative to [$(PtIMe_3)_4$]}, m.p. 98—99 °C (Found: C, 19.1, H, 4.3. $C_8H_{12}IPtS_2$ requires C, 19.1, H, 4.2%).

N.M.R. Experiments.—N.m.r. spectra were recorded on a Brüker AM250 spectrometer with an ASPECT 3000 computer. Multinuclear ^1H, ^{13}C, and ^{195}Pt spectra were obtained at respective frequencies of 250, 62.9, and 53.7 MHz. N.m.r. probe temperatures were varied and measured with the standard

Brüker accessory B-VT1000, the calibration of which was checked against a Comark type 5000 digital thermometer. Quoted temperatures are accurate to ±1 °C. Two-dimensional ^{195}Pt and ^{1}H spectra were produced using the Brüker automation programs NOESYX and NOESY respectively. The pulse sequence in both cases was D1–90°–D0–90°–D9–90°–f.i.d. (free induction decay). The initial relaxation delay time D1 was typically 2—4 s, D0 was initially 3×10^{-6} s, and D9, the mixing time τ_m, was varied according to the experimental conditions (see later). In the NOESYX program the ^{1}H decoupler was gated off during D1 and on for the remainder of the pulse sequence.

For the ^{195}Pt two-dimensional experiments, the NOESYX sequence was repeated for 128 values of D0, *i.e.* the F_1 dimension of the data table contained 128 words, which was then zero-filled to 512 words. For the ^{1}H two-dimensional experiments, the F_1 dimension contained 64 words, which was then zero-filled to 512 words. In all experiments the F_2 dimension contained 1 024 words. No random variation of D9 (τ_m) was provided since no scalar couplings were present. The number of scans per experiment was in the range 72—184 for ^{195}Pt spectra, giving a total experiment time of *ca.* 15 h. Four scans per experiment were used for the ^{1}H spectra which required a total experiment time of 0.5—1 h. Data relating to spectra at temperatures below 273 K were processed using an unshifted sine-bell window function in both dimensions. At temperatures > 273 K, the spectral lines exhibited slight exchange broadening and no window functions were used in processing their two-dimensional data. In all cases magnitude-mode spectra were calculated, followed by symmetrisation about the diagonal.

Computations.—The dynamic information contained in the cross-peak intensities of the ^{195}Pt and ^{1}H 2D-EXSY spectra was processed using the previously described[11] D2DNMR program. This requires, as input data, intensities of the diagonal and cross peaks in the two-dimensional spectra, the relative populations of the exchanging sites, and the mixing time, τ_m, in the NOESY pulse sequence. Signal intensities were measured by integrating signals on rows of the two-dimensional data table which contained the most intense slices of signals (typically three rows or more). Cross peaks between the same diagonal peaks were adjusted to the same intensity value in order that the input intensity matrix I was symmetric. The choice of optimal mixing time was based on the experience gained in the previous study of [PtXMe$_3$(MeSCH$_2$CH$_2$SMe)] (X = Cl or I)[11] where it was shown that the time should be of sufficient magnitude to give relatively strong cross peaks but not so excessively long that the signal intensities become insensitive to exchange rates, or that all signals lose appreciable intensity due to spin-lattice relaxation.

Values of T_1 were not measured for the present complex but were reasonably assumed to be very similar to the value for [PtIMe$_3$(MeSCH$_2$CH$_2$SMe)], namely *ca.* 1.5 s for ^{195}Pt nuclei at 263 K. The computer program calculates the kinetic plus relaxation matrix L, the off-diagonal elements of which give the required rate constants, k_{ij}. In the present four-site exchange problem this is a 4 × 4 matrix. The errors associated with these rate constants were calculated as described previously.[11] The k values were fairly insensitive to the choice of τ_m, the optimal values of the latter being those which produced the smallest uncertainties in the k values.

Results and Discussion

Pyramidal Sulphur Inversion.—Complexes of general type [PtXMe$_3$(MeECH$_2$CH$_2$E′Me)] (X = Cl, Br, or I; E = E′ = S or Se, E = S, E′ = Se) are known to adopt the *fac* geometry[12] and exhibit solution n.m.r. spectra at low temperatures characteristic of isomeric mixtures arising from the fixed pyramidal geometries of the co-ordinated chalcogen atoms. In the case of the dithio- and diseleno-ether complexes (E = E′ = S or Se),[13] three distinct species may be differentiated by n.m.r. at low temperatures, whereas in the mixed thio–seleno-ether complexes (E = S, E′ = Se),[14] four different invertomers arise. On raising the solution temperature of the complexes, exchange broadening and band coalescences occur due to the increasing rates of pyramidal inversion of the two chalcogen atoms. Proton n.m.r. spectra of the above species were found to be sensitive to no more than two rate constants at any temperature and so standard bandshape fitting procedures could be applied.[13,14]

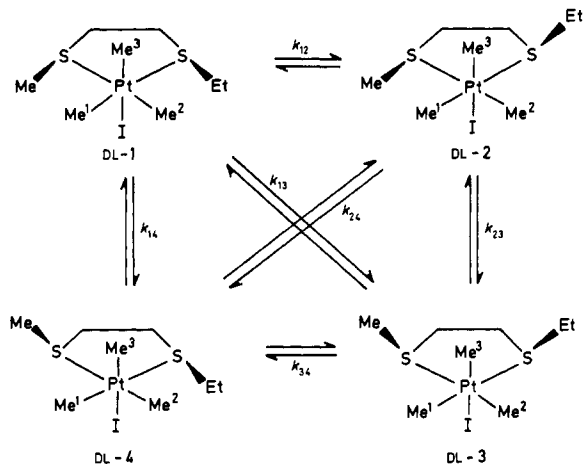

Figure 1. The four invertomers of [PtIMe$_3$(MeSCH$_2$CH$_2$SEt)] showing the single-site and double-site sulphur inversion pathways

In order to examine the effect of different alkyl substituents on the inverting chalcogen atoms we sought to study the stereodynamics of [PtIMe$_3$(MeSCH$_2$CH$_2$SEt)]. At below-ambient temperatures this complex exists in solution as a mixture of four DL invertomers, one component of each DL pair being shown in Figure 1.

The low-temperature (< *ca.* 0 °C) ^{1}H spectra contain many methylene and methyl signals with severe overlaps occurring between the ligand backbone methylene, the S-methylene, and the S-methyl signals (Figure 2). The S-methyl signals can be assigned with confidence but a full analysis was not attempted as the spectra are clearly intractable as far as d.n.m.r. studies are concerned. The low-temperature ^{13}C spectrum contains the requisite number of carbon signals (20 CH_3 and 12 CH_2) and a detailed assignment will be presented later.[15] Dynamic ^{13}C studies were also not considered a realistic possibility and attention was turned to ^{195}Pt spectroscopy. The one-dimensional ^{195}Pt spectrum of this complex consists of four signals spread over a chemical shift range of *ca.* 120 p.p.m. This spectral spread precludes one-dimensional bandshape studies but strongly favours 2D-EXSY experiments analogous to those carried out on [PtXMe$_3$(MeSCH$_2$CH$_2$SMe)] (X = Cl or I).[11]

Two-dimensional ^{195}Pt 2D-EXSY spectra were therefore obtained in the temperature range 223—293 K. At all temperatures within this range the four ^{195}Pt signals were clearly defined and experienced slight exchange broadening, due to S inversion, only at temperatures above 273 K. Chemical shifts and relative signal intensities (invertomer populations) are listed in Table 1 and a typical two-dimensional contour plot (with the one-dimensional spectrum along the upper edge of the plot) is shown in Figure 3. The assignment of the signals was based on the known assignment of [PtIMe$_3$(MeSCH$_2$CH$_2$SMe)].[11] (The accidental presence of the latter complex as an

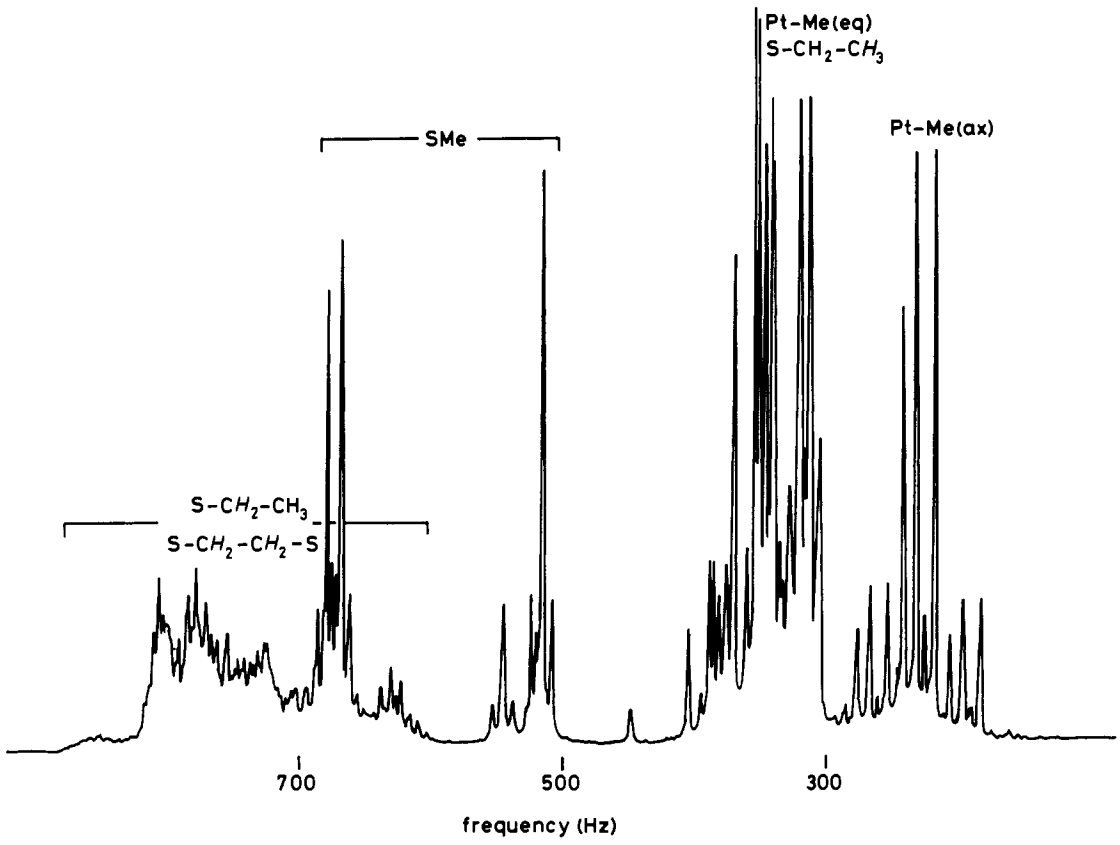

Figure 2. ^{1}H N.m.r. spectrum (250-MHz) of [$PtIMe_3(MeSCH_2CH_2SEt)$] ($CDCl_3$ solution, 253 K) showing partial assignments

impurity in the title complex proved a useful assignment aid.) Distinction between the DL-2 and DL-4 shifts was based on the relative populations of these two species. In the DL-2 species the S-ethyl group experiences more severe steric interaction with the axial Pt-methyl than does the S-methyl in the DL-4 species and therefore the latter is preferred over DL-2. It is also noteworthy that the *X*-ray crystal structure of [$PtClMe_3(MeSCH_2CH_2SEt)$][15] also indicates the DL-4 conformation. This conformation is clearly becoming dominant at low temperatures in the present iodide complex where the population increase is at the expense of the DL-1 species population. Thus, at 223 K the invertomer populations are in the order DL-4 > DL-2 > DL-1 > DL-3, in contrast to the order DL-1 > DL-4 > DL-2 > DL-3 at 293 K. Temperature dependences of the ^{195}Pt chemical shifts (Table 1) are consistently similar for all invertomers, shifts having positive (*i.e.* high frequency) temperature coefficients of *ca.* 0.3 p.p.m. K^{-1}.

Platinum-195 2D-EXSY spectra in the temperature range 233—298 K were obtained using the mixing times given in Table 2. These values were chosen in accordance with the criteria discussed in the Experimental section. Cross peaks were detected between the four diagonal peaks in all spectra between 233 and 288 K. In the spectra measured at 293 and 298 K, exchange broadening prevented the detection of the DL-3 signal and so rate constants to or from this invertomer could not be established. Rate constants were calculated using the D2DNMR program[11] and their values plus uncertainties, collated in Table 2, merit careful scrutiny. The reproducibility of these values and their sensitivity to different mixing times were tested by carrying out three independent runs at 283 K. Values of k_{ij} are shown to be reproducible well within their experimental uncertainties, and are not particularly sensitive to chosen τ_m values. Some of our experiments have in fact shown that τ_m values may be varied by factors of two or three without significantly changing the magnitudes of the k_{ij} values, although their uncertainties increase as τ_m deviates further from its optimal value.

Table 1. Platinum-195 chemical shifts[a] and invertomer populations[b] of [$PtIMe_3(MeSCH_2CH_2SEt)$]

	DL-1		DL-2		DL-4		DL-3	
T/K	δ	*p*	δ	*p*	δ	*p*	δ	*p*
223	1 076.8	22.0	1 026.5	28.6	1 009.8	37.8	960.1	11.7
233	1 079.7	24.0	1 029.8	27.6	1 012.9	36.7	963.5	11.6
243	1 082.2	26.0	1 031.4	27.4	1 014.5	36.1	964.6	10.5
253	1 086.1	27.8	1 035.4	27.3	1 018.4	35.2	968.5	9.7
263	1 089.4	29.5	1 037.7	26.4	1 020.6	33.8	970.2	10.2
273	1 092.7	31.2	1 040.7	26.1	1 023.6	33.6	973.0	9.1
283	1 096.5	32.9	1 043.9	25.7	1 026.8	33.2	976.0	8.2
293	1 100.7	33.1	1 048.0	25.4	1 030.8	32.3	980.4	9.2

[a] Shifts (δ) relative to Ξ = 21.4 MHz. [b] Populations (*p*) given as percentages.

The most important conclusion to be drawn from the data in Table 2 is that values of k_{12}, k_{14}, k_{23}, and k_{34} all increase steadily with temperature whereas k_{13} and k_{24} values stay around zero, their uncertainties in most cases being greater than their absolute values. This means that single-site sulphur inversion is occurring at n.m.r.-measureable rates whereas synchronous double sulphur inversion (as represented by k_{13}

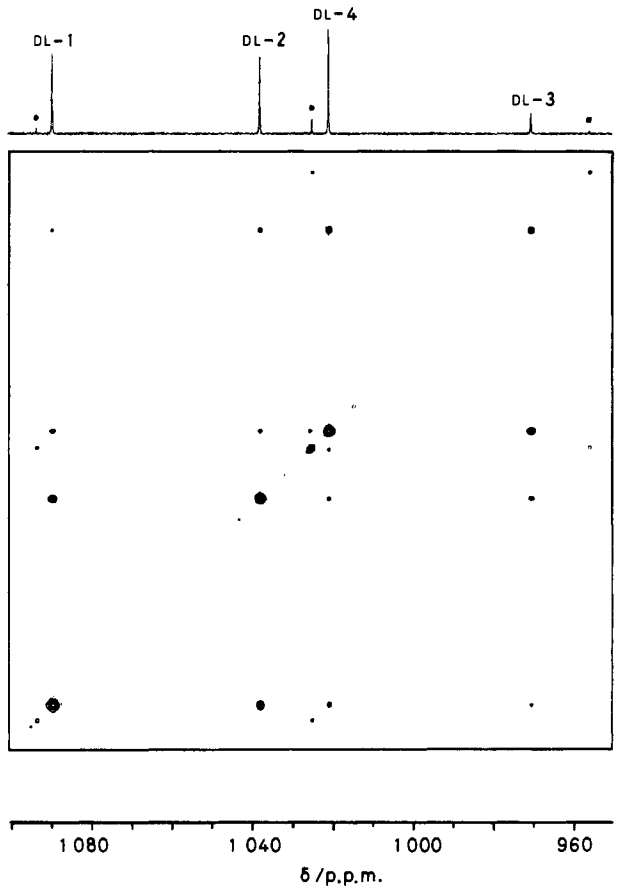

Figure 3. ^{195}Pt 2D-EXSY spectrum of [$PtIMe_3(MeSCH_2CH_2SEt)$] ($CDCl_3$ solution, 263 K, τ_m = 0.08 s). Signals marked (*) are due to a small amount of [$PtIMe_3(MeSCH_2CH_2SMe)$]

and k_{24}) is immeasurably slow in this temperature range. This conclusion validates the assumptions that have been made previously in one-dimensional bandshape fittings of these mononuclear platinum(IV) complexes.[1,13,14] While one-dimensional n.m.r. bandshape studies had shown previously that single-site inversion of chalcogen atoms was dominant, possible combinations of single- and double-site inversion mechanisms could not be excluded with certainty. The two-dimensional approach to multi-site dynamic problems is therefore much more definitive, *providing* two-dimensional spectra are interpreted *quantitatively*. In the present work, cross peaks were detected between DL-1 and DL-3, and between DL-2 and DL-4 species, even though the rate constants for these direct exchanges were shown to be negligibly small. These second-order cross peaks have been noted previously,[16] and illustrate the important fact that the existence of a cross peak in a two-dimensional n.m.r. exchange spectrum does *not* necessarily imply a direct exchange pathway between the pair of sites in question. This point should not be overlooked when attempting to differentiate between various exchange pathways by qualitative interpretation of two-dimensional spectra.

A stringent test of the correctness of these rate constants derived by two-dimensional n.m.r. was performed by using the sets of values from the ^{195}Pt two-dimensional spectra at 273 and 283 K to fit portions of the one-dimensional ^{1}H spectra. The S-methyl region was chosen for fitting because the chemical shifts of the four SMe signals were known and signal overlap was less severe than in other regions. Figure 4 shows the exchange-broadened experimental ^{1}H spectrum at 273 K together with the computer-simulated spectrum using the rate constants in Table 2. Considering the uncertainties of some of these k_{ij} values, the agreement is very acceptable. Furthermore, it illustrates the superiority of the two-dimensional approach over one-dimensional bandshape analysis, since without prior knowledge of these six rate constants, it would have been quite impossible to have fitted this spectrum to a unique set of these six variables.

Table 2. Exchange rate constants derived from ^{195}Pt 2D-EXSY spectra of [$PtIMe_3(MeSCH_2CH_2SEt)$]

T/K	τ_m/s	k_{12}/s^{-1}	k_{13}/s^{-1}	k_{14}/s^{-1}	k_{23}/s^{-1}	k_{24}/s^{-1}	k_{34}/s^{-1}
233	0.8	0.08 ± 0.02	0.0004 ± 0.02	0.01 ± 0.02	0.02 ± 0.02	−0.0006 ± 0.2	0.22 ± 0.04
243	0.3	0.31 ± 0.04	0.016 ± 0.04	0.07 ± 0.04	0.09 ± 0.04	−0.003 ± 0.04	0.97 ± 0.12
253	0.3	1.15 ± 0.08	0.018 ± 0.08	0.28 ± 0.06	0.30 ± 0.09	0.014 ± 0.06	3.22 ± 0.35
263	0.08	3.85 ± 0.28	−0.001 ± 0.25	0.99 ± 0.21	1.17 ± 0.31	0.11 ± 0.23	10.8 ± 1.1
268	0.05	6.03 ± 0.54	−0.18 ± 0.48	1.31 ± 0.39	1.62 ± 0.60	0.39 ± 0.45	17.3 ± 2.3
273	0.027	11.3 ± 1.0	−0.04 ± 0.80	2.87 ± 0.68	2.74 ± 1.04	0.41 ± 0.79	27.6 ± 3.7
278	0.02	17.9 ± 1.8	−1.0 ± 1.6	5.3 ± 1.4	3.0 ± 2.1	1.5 ± 1.6	63.6 ± 11.1
283	0.011	29.2 ± 3.3	0.3 ± 2.6	7.1 ± 2.2	5.9 ± 3.6	4.9 ± 2.7	91.1 ± 22.4
283	0.015	28.1 ± 3.3	−1.7 ± 2.6	8.0 ± 2.2	7.3 ± 3.7	0.8 ± 2.8	78.8 ± 24.7
283	0.015	28.7 ± 3.3	−1.2 ± 2.6	8.8 ± 2.2	6.2 ± 3.7	0.9 ± 2.8	94.2 ± 24.7
288	0.01	47.6 ± 7.0	−1.4 ± 7.4	12.9 ± 6.2	7.5 ± 9.9	3.6 ± 7.9	185 ± 71
293	0.005	74 ± 15	1.6 ± 12.3	16.3 ± 10.0		10.1 ± 12.9	223 ± 79
298	0.005	126 ± 40		32.2 ± 33.5		9.1 ± 53.8	

Table 3. Arrhenius and Eyring energy data for sulphur pyramidal inversion in [$PtIMe_3(MeSCH_2CH_2SEt)$]

	S-ethyl		S-methyl	
Parameter	DL-1 ⟶ DL-2	DL-3 ⟶ DL-4	DL-1 ⟶ DL-4	DL-2 ⟶ DL-3
E_a/kJ mol^{-1}	65.2 ± 0.4	66.4 ± 1.2	68.0 ± 1.4	60.1 ± 2.1
$\log_{10}(A/s^{-1})$	13.5 ± 0.4	14.2 ± 0.2	13.4 ± 0.3	11.9 ± 0.4
$\Delta G^{\ddagger}$/kJ mol^{-1}	61.10 ± 0.04*	58.2 ± 0.1*	64.4 ± 0.2*	65.4 ± 0.3*
$\Delta H^{\ddagger}$/kJ mol^{-1}	63.0 ± 0.4	64.3 ± 1.1	65.8 ± 1.4	57.9 ± 2.2
$\Delta S^{\ddagger}$/J K^{-1} mol^{-1}	6.4 ± 1.3	20.3 ± 4.3	4.8 ± 5.3	−24.9 ± 8.2

* Data refer to 298.15 K.

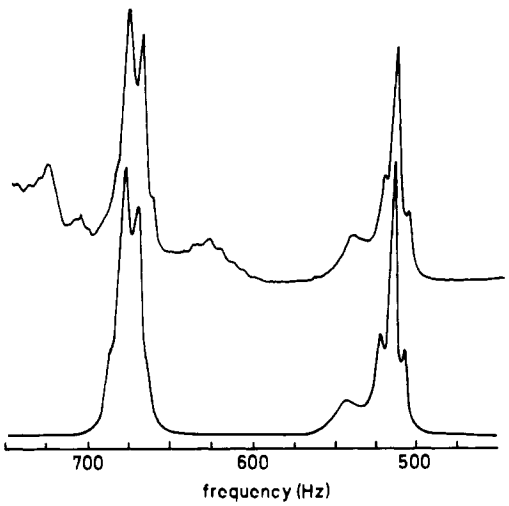

Figure 4. Experimental ^{1}H n.m.r. spectrum (250 MHz) of [$PtIMe_3$-($MeSCH_2CH_2SEt$)] at 273 K showing the exchange-broadened S-methyl signals, compared to the computer-simulated spectrum based on the rate constants derived from the ^{195}Pt 2D-EXSY spectrum (k_{12} = 11.3, k_{14} = 2.87, k_{23} = 2.74, k_{34} = 27.6, k_{13} = k_{24} = 0.001 s^{-1}). Additional signals appear in the experimental spectrum due to -SCH_2CH_2S- and -SCH_2CH_3 resonances

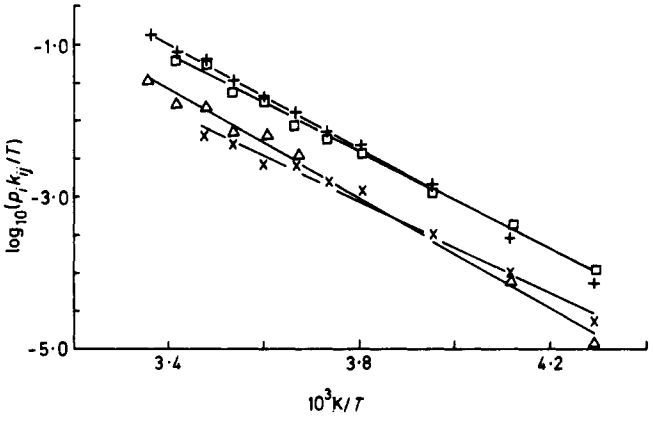

Figure 5. Eyring plots using population-weighted rate data p_ik_{ij} showing the different energies of S-methyl and S-ethyl pyramidal inversion. Legend for data points: S-ethyl, DL-1 ⟶ DL-2 (+), DL-3 ⟶ DL-4 (□); S-methyl, DL-1 ⟶ DL-4 (△), DL-2 ⟶ DL-3 (×)

The temperature dependences of the rate constants, k_{12}, k_{14}, k_{23}, and k_{34} were plotted according to the Arrhenius and Eyring rate theories and the results are given in Table 3. The $\Delta G^{\ddagger}$ values, being least prone to systematic error, provide the clearest description of the relative sulphur inversion energies. These clearly fall into two groups, namely 58.2 and 61.1 kJ mol^{-1} for S-ethyl inversion and 64.4 and 65.4 kJ mol^{-1} for S-methyl inversion. This alkyl dependence is shown strikingly in the Eyring graphs (Figure 5) based on population-weighted rate constants p_ik_{ij}. Examination of the Eyring equation shows that the vertical separation of pairs of lines in the two groups is equal to the term $-\Delta(\Delta G^{\ddagger})/2.303\ RT$, where $\Delta(\Delta G^{\ddagger})$ is a measure of the difference in energies of S-methyl and S-ethyl pyramidal inversions. For the four invertomers in question these differences range from 3.3 to 7.2 kJ mol^{-1}, S-ethyl inversion always being associated with the lower energy. This finding is in accordance with studies of steric effects on nitrogen inversion

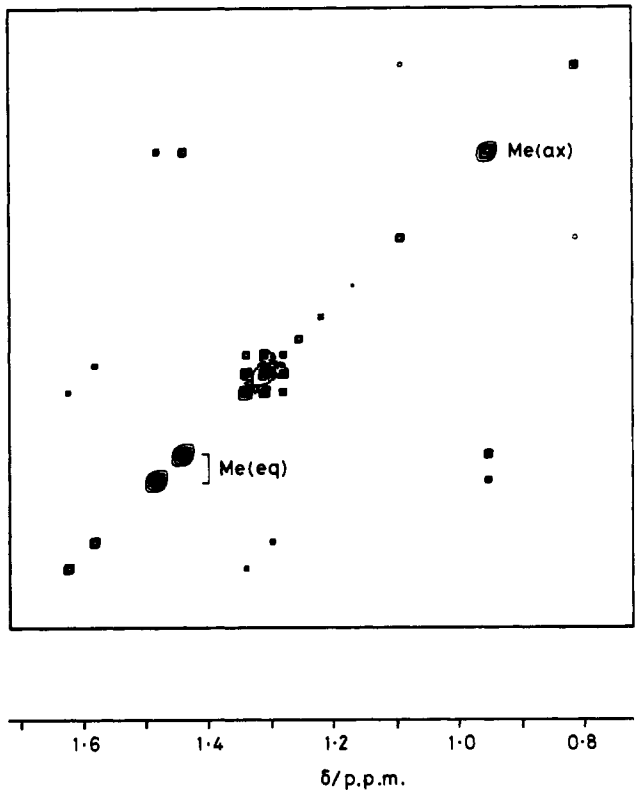

Figure 6. ^{1}H 2D-EXSY spectrum of [$PtIMe_3(MeSCH_2CH_2SEt)$] showing the Pt-methyl signals plus ^{195}Pt satellites (plus S-CH_2CH_3 triplet). Note the additional cross peaks of the ^{195}Pt satellites. Experimental conditions: CD_2Cl_2 solution, 338 K, τ_m = 1.0 s

barriers.[17,18] Early work on *N*-alkylaziridines[19,20] indicated that replacement of a small alkyl group by a bulkier group would lead to a lower N inversion barrier since the ground-state steric strain would be relieved somewhat in the transition state, the energy of which (relative to the ground state) would be less than for a less sterically hindered compound. Numerous other studies on N inversion have confirmed this trend although the inversion energies quoted should be treated with caution as, in most cases, they are based on band coalescence measurements. Apart from some very recent work on [$W(CO)_4(RSCH_2CH_2SR)$] (R = Me, Et, Pr^i, or Bu^t) complexes,[21] we are not aware of comparable data for pyramidal sulphur inversion and certainly a direct comparison of S-methyl and S-ethyl inversion *in the same molecule* has not been reported previously. Our activation energy data therefore provide the most accurate description to date of alkyl dependence of S inversion barriers.

High-temperature Ligand Fluxions.—On raising the temperature of solutions of complexes [$PtXMe_3(MeECH_2CH_2E'Me)$] (X = Cl, Br, or I; E = E' = S or Se, E = S, E = Se),[1,14] exchange broadening and eventual coalescence of the Pt-methyl ^{1}H signals is known to occur as a result of exchange of Pt-methyl environments. This has been interpreted[14] as arising from a 180° 'pancake' rotation of the ligand followed by a scrambling of the Pt-methyl groups. Direct evidence for this ligand rotation movement and the extent to which it is correlated to the Pt-methyl movement has been hard to achieve to date. It was therefore hoped that a ^{1}H 2D-EXSY study of the Pt-methyl region of [$PtIMe_3(MeSCH_2CH_2SEt)$] would provide a definitive explanation of the fluxional mechanism.

Proton 2D-EXSY spectra were therefore recorded in the temperature range 333—378 K, where exchange broadening

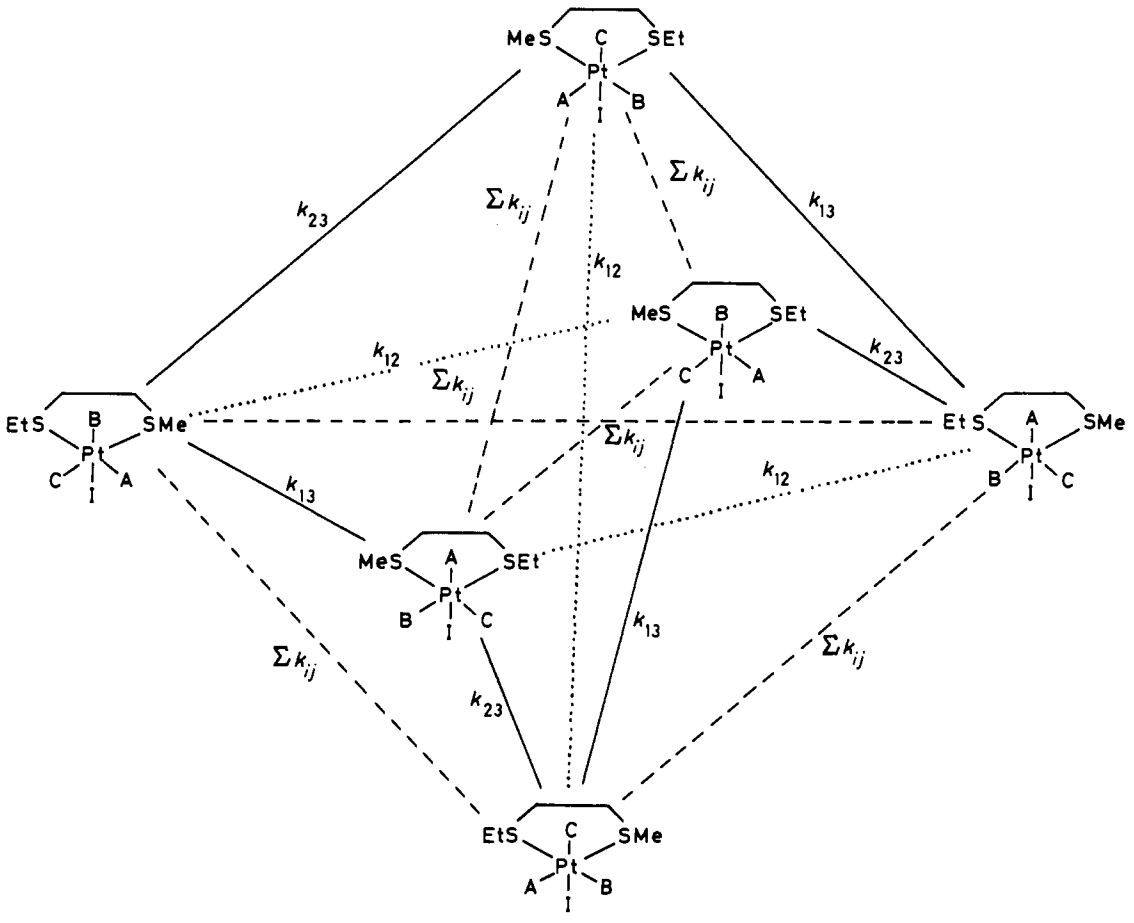

Figure 7. Graph diagram showing the interconversion pathways of the six permutation isomers of [$PtIMe_3(MeSCH_2CH_2SEt)$]. Pathways are defined as (——) correlated ligand (180°)/$PtMe_3$ (120°) rotations, (– – –) $PtMe_3$ rotations (120°), (· · ·) ligand rotations (180°). Rate constants are defined according to the Pt-methyl labelling in Figure 1. Note that a similar graph diagram exists for the mirror images of these structures

Table 4. Ligand/$PtMe_3$ rotation rate constants for [$PtIMe_3(MeSCH_2CH_2SEt)$]

T/K	τ_m/s	k_{12}^{Me}/s^{-1}	k_{13}^{Me}/s^{-1}	k_{23}^{Me}/s^{-1}
338	1.0		0.073 ± 0.016	0.138 ± 0.018
343	1.0		0.144 ± 0.021	0.270 ± 0.025
343	1.0	0.037 ± 0.017	0.158 ± 0.021	0.243 ± 0.025
348	1.0	0.042 ± 0.022	0.251 ± 0.028	0.453 ± 0.039
353	0.8	0.17 ± 0.04	0.470 ± 0.051	0.83 ± 0.08
353	0.8	0.18 ± 0.04	0.492 ± 0.051	0.81 ± 0.08
358	0.4	0.15 ± 0.05	0.790 ± 0.07	1.36 ± 0.10
363	0.2	0.61 ± 0.10	1.59 ± 0.13	2.83 ± 0.18
363	0.2	0.52 ± 0.10	1.46 ± 0.13	2.40 ± 0.18
368	0.1	0.49 ± 0.14	2.19 ± 0.18	3.77 ± 0.25
373	0.05	1.6 ± 0.3	3.9 ± 0.3	7.4 ± 0.4
373	0.05	1.4 ± 0.3	3.6 ± 0.3	6.1 ± 0.4
378	0.04	1.6 ± 0.3	5.1 ± 0.4	7.5 ± 0.5

Table 5. Arrhenius and Eyring energy data for ligand/$PtMe_3$ rotation in [$PtIMe_3(MeSCH_2CH_2SEt)$]

Parameter	eq_1–eq_2	ax–eq_1	ax–eq_2
E_a/kJ mol^{-1}	126.0 ± 10.8	114.1 ± 2.2	112.0 ± 3.0
$\log_{10}(A/s^{-1})$	17.8 ± 1.6[a]	16.6 ± 0.3[a]	16.5 ± 0.4[a]
$\Delta G^{\ddagger}$/kJ mol^{-1}	97.7 ± 1.9[b]	92.6 ± 0.4[b]	90.9 ± 0.5[b]
$\Delta H^{\ddagger}$/kJ mol^{-1}	123.0 ± 10.8	111.2 ± 2.2	109.0 ± 3.0
$\Delta S^{\ddagger}$/J K^{-1} mol^{-1}	85.0 ± 30.0[a,c]	62.2 ± 6.1[a]	60.7 ± 8.4[a]

[a] These abnormally high values are attributed to the rather narrow temperature range over which measurements were possible. [b] Data refer to 298.15 K. [c] Interpretation in terms of a dissociative process is tempting, but considered unlikely.

was minimal. A typical two-dimensional plot is shown in Figure 6. The diagonal signals consist of the three Pt-methyl signals with δ values of *ca.* 0.95 (axial), 1.44 (equatorial), and 1.48 (equatorial). Assignments of the two equatorial Pt-methyl signals are uncertain but it is assumed that the more highly shielded of the two is due to the group on the S-ethyl side of the molecule. Platinum-195 satellite signals are also present with $^2J(PtH_{ax})$ = 69.9 and $^2J(PtH_{eq})$ = 70.8 Hz at 333 K. The spectrum also contains a triplet signal from the methyl protons of the S-ethyl group. Cross peaks were detected between the three Pt-methyl signals and relative intensities of all nine signals carefully measured. The pairs of ^{195}Pt-satellites of each Pt-methyl signal also showed cross peaks within each pair, but these contained no exchange information and were related to the relaxation rate of the ^{195}Pt nucleus. The Pt-methyl cross-peak intensities were due solely to methyl scrambling and contained no ^{1}H–^{1}H nuclear Overhauser effect contributions, since, at low temperatures (< *ca.* 333 K) where no scrambling occurs, no cross peaks were detectable.

From the intensities of these cross peaks, three exchange rate constants were obtained for each temperature, namely k_{12}^{Me}, k_{13}^{Me}, and k_{23}^{Me} (Table 4). The labelling refers to Figure 1, where it will be noted that k_{12}^{Me} refers to eq–eq methyl exchange, and k_{13}^{Me} and k_{23}^{Me} to ax–eq methyl exchanges. Arrhenius and Eyring activation energies were computed in the usual way and results tabulated (Table 5). These values are notable in a number of respects. First, the rates of all three types of methyl–methyl exchange are measurably different at any given temperature, the rate of eq–eq exchange being noticeably lower than the rates of ax–eq exchange. The activation energies (as expressed by $\Delta G^{\ddagger}$ values) reflect these differences. The values based on ax–eq exchanges are similar in magnitude to the 'methyl scrambling' energies reported for related platinum(IV) chelate complexes, namely $[PtXMe_3(MeSZSeMe)]$ (X = Cl, Br, or I; Z = $-CH_2CH_2-$ or o-C_6H_4)[14] and $[PtXMe_3(MeSCH_2CH_2S\text{-}Me)]$ (X = Cl, Br, or I).[22] In the above complexes, however, it was possible to report only a single fluxion energy since in these cases the two equatorial Pt-methyl signals were either isochronous[22] due to the symmetry of the complex or insufficiently anisochronous[14] for the one-dimensional proton spectrum to depend on the rate of eq–eq exchange. Our energy data for $[PtIMe_3(MeSCH_2CH_2SEt)]$ however, enable us to inquire closely into the possible mechanism(s) of its fluxionality.

Ligand 180° 'pancaking' will cause an exchange between the two equatorial Pt-methyls, Me^1 and Me^2, leaving the axial Me^3 unaffected. Scrambling of the Pt-methyl environments either by a random mechanism or some type of concerted movement will exchange all three methyl sites. Therefore, any *uncorrelated* combination of these processes will result in the rate of eq–eq exchange at any temperature being greater than ax–eq exchanges. This is precisely *opposite* to what is observed and so the case for correlation between ligand rotations and exchange of the Pt-methyls must be carefully examined. This is a most reasonable possibility since the energies of these two types of fluxions are known to be very similar.[22]

Since Pt-methyl bond breaking does *not* occur, we suggest that exchange of the axial and equatorial Pt-methyl environments be explained in terms of rotations of the Pt–Me_3 moiety. If 180° ligand rotations are precisely correlated with 120° rotations of the Pt–Me_3 moiety about its C_3 axis, then no net eq–eq methyl exchange will occur. This is most easily visualised by considering the interconversion of the six permutational isomers of the complex under conditions of rapid sulphur inversion. These are shown in Figure 7 where the Pt-methyls are labelled A, B, and C, and the rate constants refer to the Pt-methyl labelling in Figure 1.

Correlated ligand (180°)/$PtMe_3$ (120°) rotations interconvert all six species with rate constants k_{13} and k_{23} depending on which equatorial Pt-methyl is exchanged in a particular step. It would appear that these pathways are energetically most favoured. However, some direct eq–eq methyl exchange does occur, albeit at quite slow rates (Table 4) so that the other pathways in Figure 7 must also be traversed but with somewhat lower probabilities. In other words, the measured rate constants suggest a strongly correlated ligand (180°)/$PtMe_3$ (120°) rotation, but with some uncorrelated movements of these different parts of the complex. It is not possible to decide whether the highest energy fluxion, based on the k_{12} values, is due solely to ligand rotation or $PtMe_3$ rotation or some uncorrelated combination of both. Neither is it possible to say much about the likely transition-state structures of these interconversions. Different transition states can be visualised depending on the direction of rotation of the ligand and whether the $PtMe_3$ cone angle changes appreciably during the rotation. Despite these outstanding questions, the two-dimensional n.m.r. rate data clearly establish the dominant fluxional mechanism in this mononuclear platinum(IV) complex. Such a conclusion is closely analogous to that reached for dinuclear platinum(IV) complexes of the type $[(PtXMe_3)_2(SCH_2SCH_2SCH_2S\overline{CH_2})]$ (X = Cl, Br, or I)[23] and $[(PtXMe_3)_2\{HC(SMe)_2\}]$ (X = Cl or Br).[24]

This detailed two-dimensional n.m.r. study of a single compound has established reliable numerical values (and their temperature dependences) of nine distinct rate constants associated with the extensive fluxionality in this platinum(IV) complex. It demonstrates the power of two-dimensional exchange spectroscopy for probing complex stereochemical non-rigidity.

References

1 E. W. Abel, S. K. Bhargava, and K. G. Orrell, *Prog. Inorg. Chem.*, 1984, **32**, 1.
2 J. Sandstrom, 'Dynamic NMR Spectroscopy,' Academic Press, London, 1982.
3 S. Forsén and R. A. Hoffman, *Prog. Nucl. Magn. Reson. Spectrosc.*, 1966, **1**, 173.
4 B. E. Mann, *J. Magn. Reson.*, 1976, **21**, 18; 1977, **25**, 91; *J. Chem. Soc., Perkin Trans. 2*, 1977, 84.
5 J. Jeener, B. H. Meier, P. Bachmann, and R. R. Ernst, *J. Chem. Phys.*, 1979, **71**, 4546.
6 S. Macura and R. R. Ernst, *Mol. Phys.*, 1980, **41**, 95.
7 H. Gesmar and J. J. Led, *J. Magn. Reson.*, 1986, **68**, 95
8 M. Grassi, B. E. Mann, B. T. Pickup, and C. M. Spencer, *J. Magn. Reson.*, 1986, **69**, 92.
9 C. L. Perrin and R. K. Gipe, *J. Am. Chem. Soc.*, 1984, **106**, 4036.
10 E. R. Johnston, M. J. Dellwo, and J. Hendrix, *J. Magn. Reson.*, 1986, **66**, 399.
11 E. W. Abel, T. P. J. Coston, K. G. Orrell, V. Šik, and D. Stephenson, *J. Magn. Reson.*, 1986, **70**, 34.
12 E. W. Abel, A. R. Khan, K. Kite, K. G. Orrell, and V. Šik, *J. Chem. Soc., Dalton Trans.*, 1980, 1169.
13 E. W. Abel, A. R. Khan, K. Kite, K. G. Orrell, and V. Šik, *J. Chem. Soc., Dalton Trans.*, 1980, 1175.
14 E. W. Abel, S. K. Bhargava, K. Kite, K. G. Orrell, V. Šik, and B. L. Williams, *J. Chem. Soc., Dalton Trans.*, 1982, 583.
15 E. W. Abel, I. Moss, K. G. Orrell, V. Šik, D. Stephenson, P. A. Bates, and M. B. Hursthouse, *J. Chem. Soc., Dalton Trans.*, in the press.
16 C. Wynants, G. Van Binst, C. Mügge, K. Jurkschat, A. Tzschach, H. Pepermans, M. Gielen, and R. Willem, *Organometallics*, 1985, **4**, 1906.
17 A. Rauk, L. C. Allen, and K. Mislow, *Angew. Chem., Int. Ed. Engl.*, 1970, **9**, 400.
18 I. O. Sutherland, *Annu. Rev. NMR Spectrosc.*, 1971, **4**, 71.
19 A. T. Bottini and J. D. Roberts, *J. Am. Chem. Soc.*, 1958, **80**, 5203.
20 F. A. L. Anet and J. M. Osyany, *J. Am. Chem. Soc.*, 1967, **89**, 352.
21 E. W. Abel, I. Moss, K. G. Orrell, and V. Šik, *J. Organomet. Chem.*, in the press.
22 E. W. Abel, M. Z. A. Chowdhury, K. G. Orrell, and V. Šik, *J. Organomet. Chem.*, 1983, **258**, 109.
23 E. W. Abel, G. D. King, K. G. Orrell, V. Šik, T. S. Cameron, and K. Jochem. *J. Chem. Soc., Dalton Trans.*, 1984, 2047.
24 E. W. Abel, T. E. MacKenzie, K. G. Orrell, and V. Šik, *J. Chem. Soc., Dalton Trans.*, 1986, 2173.

Received 22*nd October* 1986; *Paper* 6/2061